Biochemical and Biophysical Research Communications 441 (2013) 208–213

Contents lists available at ScienceDirect

Biochemical and Biophysical Research Communications

journal homepage: www.elsevier.com/locate/ybbrc

Topographical analysis of As-induced folding of α-MT1a

Gordon W. Irvine [a], Martin J. Stillman [a,b,*]

[a] Department of Chemistry, The University of Western Ontario, London, Ontario N6A 5B7, Canada
[b] Department of Biology, The University of Western Ontario, London, Ontario N6A 5B7, Canada

ARTICLE INFO

Article history:
Received 8 October 2013
Available online 16 October 2013

Keywords:
Metallothionein
Metal induced folding
Protein structure
Cysteine modification
Molecular dynamics simulation
Electrospray ionization mass spectrometry

ABSTRACT

Metallothionein binds multiple metals into two clustered domains. While the structure of the fully metalated protein is well known for the Cd- and Zn-containing protein, there is little known about the structures of the metal-free protein (apo-metallothionein) and even less about the partially metalated forms. However, the partially-metalated species are vitally important intermediates in the passage of the protein from translational synthesis to its homeostatic buffer or metal chaperone roles. Because multiple metals bind to metallothioneins, the partially-metalated species span a wide range depending on the metal bound. Up to 3 As^{3+} bind stepwise to the α-domain fragment in a manner that allows measurement of each of the 4 species simultaneously with the number of free cysteines diminishing by 3 for every As^{3+} bound: apo- (11 Cys), As_1- (8 Cys), As_2- (5 Cys) and As_3-α-MT (2 Cys). The cysteine modifier benzoquinone (Bq), was used to determine the relative accessibility of the free cysteines in the α-MT fragment as a function of the number of As^{3+} bound. The effect of each As^{3+} was to induce folding in the protein. The ESI-MS results show that the whole protein folds significantly even when just one of the three As^{3+} has bound. The profile of the Bq reacting with the unbound cysteines shows effects of steric hindrance in slowing down the reaction. By freezing the reaction midway to the endpoint, the mass spectral data show the 'mid-flight' concentrations of all the key species, 27 in all. Analysis of this mid-flight reaction profile gives insight into the topology of the partially metalated MT from the differential access to the unbound cysteinyl thiols by the Bq. Significantly, the metal-free, apo-α-MT also adopts a folded structure in the presence of the As^{3+} even though there is no As^{3+} bound. This can only happen if the apo-protein wraps around other metalated proteins in solution via protein–protein interactions.

1. Introduction

Metallothionein (MT) has long been known to be a major player in cellular metal homeostasis and since its first isolation in 1957, has been shown to affect many cellular processes [1]. It is a uniquely structured protein with cysteine accounting for approximately 30% of its total residues with a mass of approximately 6–10 kDa depending on the isoform. The X-ray determined structure of the fully metalated MT resembles that of a dumbbell with two metal binding domains (named alpha and beta), separated by a short linker sequence [2,3]. The formal structure of MT is based almost entirely on the changes induced by metal coordination and the formation of the metal clusters [4,5]. However, the structure of the partially metalated protein is unknown yet is important as an intermediate in vital cellular metalation chemistries. The structure of partially metalated α-MT is addressed in the studies reported in this paper.

MT is a multi functional protein acting as a source of reducing -SH groups in redox reactions, detoxifying heavy metals and regulating cellular Zn and Cu concentrations [6]. The importance of MT to cellular metal homeostasis is highlighted by its ubiquitous nature; nearly all organisms have some type of MT or MT-like protein coded for in their genomes. In addition to the regular functions of MT, it has emerged that MT can play a role in cancer progression and drug resistance in tumors [7,8]. With many cancer treatments relying on metal based drugs, it is important to determine the mechanism by which MT metalates and the structure of the apo and partially metalated forms of MT that exist in the early stages of metalation. By studying the structure of the metal-free protein and its partially metalated intermediates, predictions about metalation with a wide variety of metals and metal complexes can be made. This may prove useful in designing drugs to combat tumours that have shown resistance to traditional therapies and in determining how MT carries out its many biological functions.

Partially metalated MT (that is MT with fewer metals bound than its maximum capacity) is vital to metal based cellular chemistry because this species is likely to be the dominant form of cellular MT. It has been considered that apo-MT does not have structure in the traditional sense but rather it adopts a more

* Corresponding author at: Department of Chemistry, The University of Western Ontario, London, Ontario, N6A 5B7 Canada. Fax: +1 519 661 3022.
E-mail addresses: martin.stillman@uwo.ca, stillman@uwo.ca (M.J. Stillman).
URL: http://www.stillmangroup.ca (M.J. Stillman).

0006-291X/$ - see front matter © 2013 Elsevier Inc. All rights reserved.
http://dx.doi.org/10.1016/j.bbrc.2013.10.044

randomly coiled and ill-defined conformation [9]. However, more recent studies have suggested that apo-MT may have a loosely defined, but structurally significant conformation at neutral pH that is only lost under denaturing conditions [10,11]. Metalation of apo-MT can lead to the formation of fully metalated protein. However, due to the concentrations of metals found in a cell, it would be expected that partially metalated species would predominate [12]. Unfortunately the only well defined structure of MT is the fully metalated form [2,3,13,14]. Significantly, structures of both the partially metalated MT and apo-MT remain elusive.

In this paper, we use the differential rate of the modification of the free cysteines in the α-metal-binding fragment to probe the spatial distribution of cysteines not involved in metal binding as a function of metalation status. Benzoquinone (Bq) reacts with cysteine forming a covalent bond. This method has been previously used to quantify free thiols in MT as well as to assess the relative accessibilities of cysteines in the alpha and beta domains of MT [11,15]. The reaction profile of Bq with up to 11 cysteines in α-MT provides a clear indication of the dependence of the structure of the apo- or partially-metalated MT on the metalation status. This reaction is dependent on the variable accessibility of the unbound cysteines. Overall, the reaction profile of Bq provides a unique description of the topological distribution of free cysteine residues.

2. Materials and methods

Methods for expression and purification of the alpha domain fragment have been previously reported in more detail [16]. In brief, the α-domain of recombinant human MT isoform 1a (α-rhMT 1a) was used having the follow sequence: GSMGKAAAAC CSCCPMSCAK CAQGCVCKGA SEKCSCCKKA AAA. The expression of the recombinant protein was carried out in *Escherichia. coli* strain BL21 using the recombinant α-rhMT 1a sequence inserted into a pET29a plasmid. The plasmid also coded for an N-terminal S-tag with the sequence MKETAAAKFE RQHMDSPDLG TLVPRGS. The inclusion of an S-tag into the recombinant protein is done to stabilize the protein during purification steps and was removed via a Thrombin CleanCleave™ kit (Sigma).

To limit oxidation of the cysteinyl thiols, all solutions used were saturated with argon and evacuated before use. In addition, all solutions used in the purification process were chilled to maintain the integrity of the protein and prevent degradation. Protein solutions were stored at −20 °C in sealed vials that had been thoroughly evacuated.

Demetalation of the protein was achieved by buffer exchange with a 10 mM solution of ammonium formate, pH adjusted to 2.8. The solutions were buffer-exchanged by centrifuge in an Amicon Ultra Centrifugal Filter Tube (Millipore) with a 3 kDA MW filter. This ensured complete demetalation and maintained high concentrations of the protein.

Solutions of 150 mM para-benzoquinone (Bq, Fisher Scientific) were prepared by dissolution in 100% methanol (Caledon) and diluted to a final concentration of 15 mM in deionized water. These solutions were prepared just before they were to be used, bubbled with argon for at least 20 min, evacuated and kept on ice shielded from light until use. Solutions of 2 mM As^{3+} were prepared by dissolving As_2O_3 in conc. HCl and diluting with deionized water. The final pH of the solution was adjusted to 2.8 using NH_4OH. The solution was then saturated with argon and evacuated before use.

MT concentrations were determined by metalation of 100 μL aliquots of the apo-MT with Cd^{2+} and examination of the absorption spectrum, specifically the peak at 250 nm. The 250 nm peak corresponds to the ligand-to-metal charge transfer transition of the Cd-thiolate bond ($\varepsilon_{\alpha;250\,nm}$ = 45,000 M^{-1} cm^{-1}). Concentrations of α-rhMT 1a ranged from 30 to 60 μM in order to ensure a strong mass spectral signal for all 27 species that are formed during metalation and modification of apo-α-rhMT 1a, that is the set of As_nBq_x-α-rhMT (n = 0–2, x = 0–11) that will be simultaneously measured.

Titration of MT with As^{3+} was carried out by adding approximately 0.5 M equivalents of As^{3+} to the protein solution. The reaction of MT with As^{3+} is much slower than with metals such as Cd^{2+} or Zn^{2+}, so the reaction vials were put in an evacuator for 1 h to equilibrate. Once the system came to equilibrium, the speciation of the α-MT was checked by ESI-MS to ensure that it had been partially-metalated and a distribution of apo-, As_1- and As_2-α-rhMT existed in solution, Fig. 1A. Sequential addition of Bq to the protein solution was performed and mass spectra acquired until all the species had been fully modified (i.e. no free cysteinyl thiols remained in any of the partially metalated species). Titrations were performed at pH 2.8.

Mass spectra were measured with a microTOF II electrospray ionization time-of-flight mass spectrometer (Bruker Daltonics, Canada) in the positive ion mode. The settings of the instrument that were used have been previously described [16]. The mass spectra were analyzed using the Bruker Daltonics analysis software.

3. Results and discussion

3.1. Metalation with As^{3+} and titration with benzoquinone (Bq)

Fig. 1A shows the mass spectral data recorded following the addition 0.5 mol equivalents of As^{3+} to apo-α-MT. The deconvoluted mass spectrum of the apo-α-MT is shown in the inset of Fig. 1A. The reaction with As^{3+} resulted in a distribution of species: apo-, As_1- and As_2-α-MT with apo- being the most abundant, As_1 at approximately 65% and As_2 at approximately 15% relative abundance. After As-binding was completed, 1 mol equivalent (mol eq) of Bq was reacted with the solution shown in Fig. 1A to form the solution used in Fig. 1B. In this early stage of the Bq titration, both modified and unmodified species are clearly present in solution. When further Bq is added to the solution used in Fig. 1B for a total of ca. 6 mol eq, a much more complicated mass spectrum is recorded, Fig. 1C, with 27 individual species (Fig. 2). This is the midpoint in the reaction, with the mass spectral data complicated by the presence of both metalated and apo-species each having varying degrees of Cys modification. The identification of all 27 species is shown in Fig. 2. This spectrum illustrates beautifully the power of the ESI-MS technique in providing exquisite detail for the progress of complicated multifaceted reactions where in Fig. 1C we see each of the many components of the complete reaction. Finally the addition of excess Bq results in all free Cys being modified; greatly simplifying the spectrum, Fig. 1D. Now just three species are observed: the apo-Bq_{11}-MT, singly metalated As_1-Bq_8-MT and the doubly metalated As_2-Bq_5-MT. Thus, Fig. 1D shows the completed reaction with all the starting species' cysteines being fully modified by Bq. This complete modification rules out oxidation as a cause of the unusual pattern seen in Fig. 1C. When MT is oxidized, Cys–Cys bridges are formed and, therefore, are unreactive towards Bq. If there was oxidation in the protein solution the endpoint in the Bq titration would be changed for some proportion of the protein that had been oxidized. For example, instead of Bq_{11}-α-rhMT being an endpoint for the titration of the apo-protein, there would be a distribution of endpoints with Bq_{11}, Bq_9 and Bq_7-α-rhMT being present depending on the extent of protein oxidation. No such distribution is observed so it can be concluded that the free thiols were not cross-linked but all form covalent bonds with Bq.

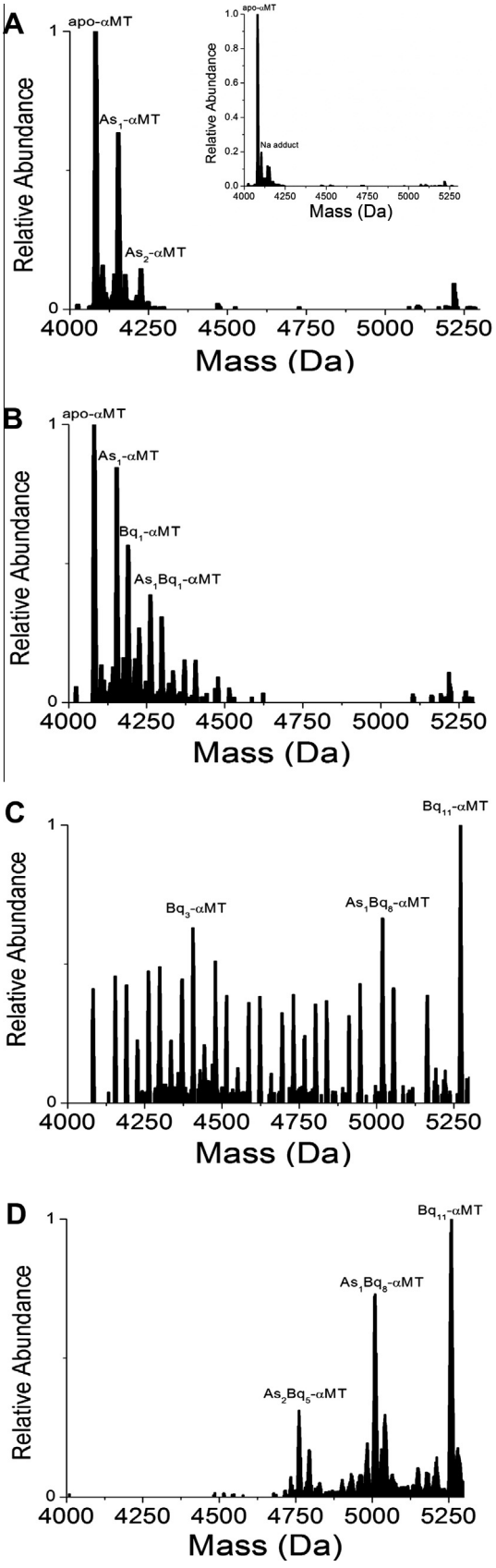

Fig. 1. Deconvoluted ESI-MS data showing the binding of As^{3+} to apo-αMT (A) and the subsequent titration of the protein solution with Bq. The spectra show the titration at approx. 0.5 (B) 5 (C) and 9 (C) molar equivalents of Bq reacted with the protein solution.

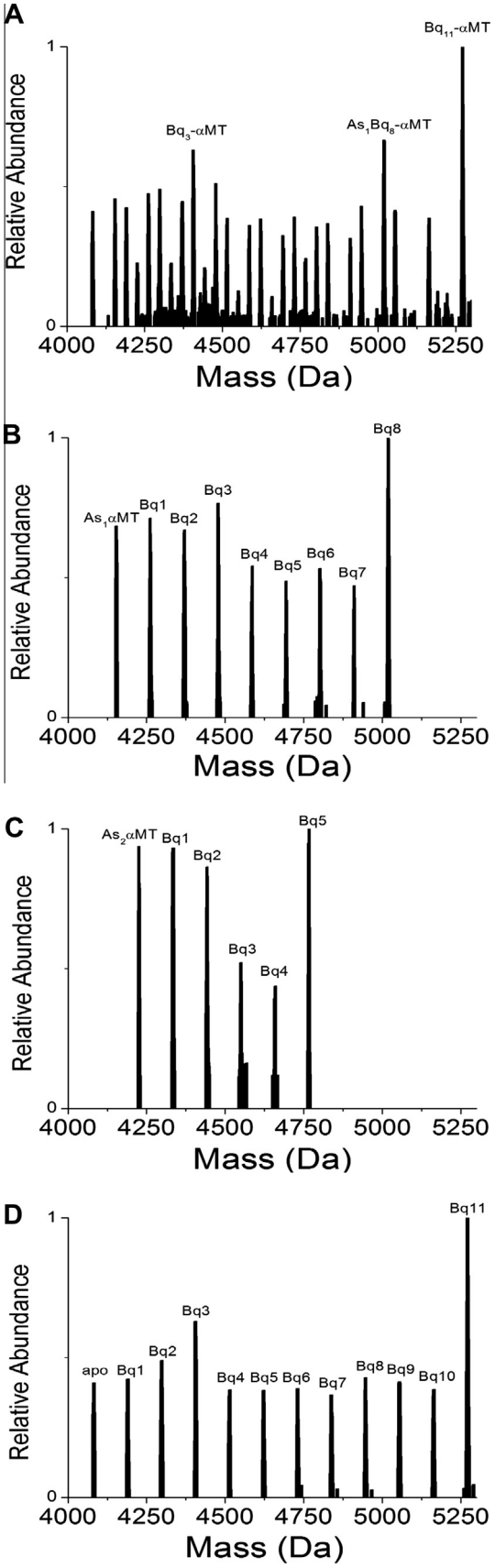

Fig. 2. Deconvoluted ESI-MS data showing the 27 individual species of intermediate and fully modified MT (A). Peaks isolated by parent species (i.e. apo-, As_1 or As_2) and shown on separate axes for clarity. The reaction profiles for As_1 (B) As_2 (C) and apo-α-MT (D).

3.2. The unusual Bq reaction profiles with apo-α-MT, As_1-α-rhMT and As_2-α-rhMT

Fig. 2A shows the ESI-mass spectrum at the midpoint of the titration (from Fig. 1C). Spectral data that includes a combination of the spectra of the apo-, As_1- and As_2-species variably modified by Bq. Figs. 2B–D separate out the three key species, namely the As_2-α-MT, the As_1-α-MT, and the apo-α-MT, and their respective cysteine-modified intermediates at this point in the reaction. We note that insufficient Bq has been added at this stage to fully modify all cysteines in the protein (that saturation point is shown in Fig. 1D). In all there are 27 individual MT species shown in this single mass spectrum. This kind of accuracy and resolution of spectral lines is unique to ESI-MS as other spectroscopic techniques would not be able to distinguish with the same detail the abundance of species present in solution. To simplify the data analysis, the spectra of the separately metalated species, along with their intermediate and final products, are isolated and are shown in Fig. 2B (As_2-α-MT + up to 5 Bq), 2C (As_1-α-MT + up to 8 Bq) and 2D (apo-α-MT + up to 11 Bq). Key in this series of spectra is that the As^{3+} can react in single steps from 1 to 3 and that it uses 3 cysteine thiols to bind. So from the 11 cysteines of apo-α-MT, there are 8 left free for As_1-, 5 left free for As_2-, and 2 left free in As_3-α-MT. When saturated with Bq, all of these free cysteines are modified (Fig. 1D, but when insufficient Bq is added the reaction stops in mid-flight providing a snapshot of the relative accessibility of the free cysteines because the reaction progress is governed by the kinetics of the modification. So, the intermediate point provides information about the dynamic structure of the protein. In the experiment carried out here that dynamic structure is controlled by the metalation status (1, 2, or 3 As^{3+}). The distribution profile of the Bq-modified cysteines depends on the relative accessibility between all 4 protein species (i.e. apo-, As_n, $n = 1, 2$ or 3).

3.3. The Bq reaction profile with As_2-α-rhMT: Fig. 2B

The profile for Bq reacting with the five free cysteines in As_2-α-rhMT is complicated. Although the Bq modification pattern reported for the apo-α-MT, namely a Normal distribution at low pH [11] is expected to be disrupted by the metalation there are no previous data to suggest what the effect of the metalation will be. Metal-induced folding has been discussed for MT for many years [17–19] and it is to be expected that with 2 As^{3+} bound that the peptide will fold and the cysteines could then be buried somewhat. The model of As_2-α-MT in Fig. 3C shows this possibility. The data in Fig. 2B suggest that the five free cysteines are differentially sterically hindered with respect to reaction with the incoming Bq. The inequivalent modification efficiencies represented by the differences in the relative fractions of the species measured reflect the differences in the relative ease of modification. The profile does not exhibit a Normal distribution rather the profile indicates that 2 of the cysteines (labeled as Bq3 and Bq4) are much less accessible and the modification reaction for these two cysteines is inefficient. The model for As_2-α-MT shown in Fig. 3C illustrates how the free cysteines can be inaccessible.

3.4. The Bq reaction profile with As_1-α-rhMT: Fig. 2C

The reaction profile of As_1-α-rhMT also follows an unusual pattern. The most abundant species is the fully modified As_2-α-MT-Bq_8, with all other species being similar with relative intensities around 0.4 (with the one exception of the Bq_3 species). This deviation from a Normal distribution indicates that the coordination of even just a single As^{3+} has altered the access to

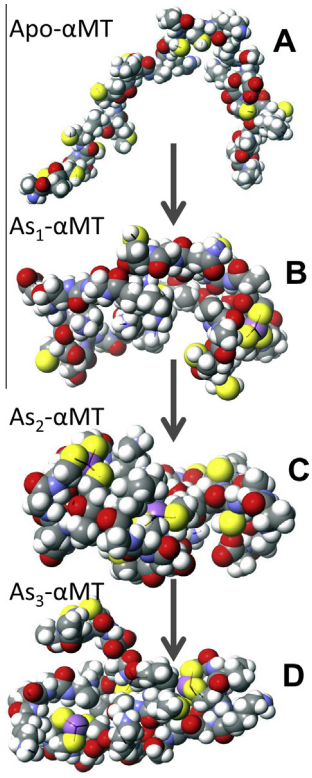

Fig. 3. Scigress models (MM3/MMD) of the structure of apo-alpha-MT (A) As_1-alpha-MT (B) As_2-alpha-MT(C) and As_3-alpha-MT (D) using space filling models to visualize the extent of folding in each species. The MD calculations were carried out at 500 K for 500 ps. The As^{3+} is shown in purple. (For interpretation of the references to colour in this figure legend, the reader is referred to the web version of this article.)

cysteines for the Bq compared with the apo-protein at low pH, most likely through structural changes induced by metal binding. This result is somewhat unexpected as, although changes in the ESI-MS charge state manifold with metalation by Cd^{2+} and Zn^{2+} were interpreted as being due to the establishment of a more compact structures [4,20], there has previously been no other evidence of folding induced by just a single metal binding. In addition, this metalation is being carried out at low pH and under low pH conditions it is expected that MT will be unfolded. As mentioned previously, MT folding is driven in large part by metal binding, so even at low pH it is reasonable to expect the formation of some metal induced structural features but the data in Fig. 2B and C suggest that all the free cysteines also fold. Even with 1 As^{3+} bound the remaining 8 free cysteine residues are clearly shielded from the solution containing Bq, thereby changing the modification profile.

The patterns observed for the modification reactions of both As_1- and As_2-α-MT can be explained by a combining the effects of two competing forces driving the Ks of each of the Bq modification reactions: (1) the initial shielding and eventual unwrapping of the protein due to the Bq modification and (2) the decrease in statistical availability of free cysteinyl thiols as the titration proceeds.

3.5. Understanding the Bq reaction profiles for As_1-α-rhMT and As_2-α-rhMT

The reaction profiles of the metalated species are similar in that there is a broad distribution of modified cysteines rather than a Normal distribution. Each modification reaction alters the structure of the protein and is likely that any structure present prior

to the reaction is changed by increasing the extent of Bq modification. The unwrapping of the protein structure exposes more cysteine residues to the solution on the surface of the protein and increases the rate of reaction with Bq. On the other hand, even as this region of the protein is unfolding because of modification reactions, fewer free cysteines exist that can be modified, making subsequent modifications statistically less likely, reducing the rate of reaction. From the increased abundance of the fully modified species in Fig. 2 B and C it is likely that the accessibility of the solvent to the free thiols is the more dominant force. The final Bq modification reaction would have a higher *K* value and this would cause the increase in abundance. The final reaction is fast due to the final free thiol being so exposed that it is more likely to come in contact with a Bq molecule than a free thiol in the folded structure of the protein in the absence of modifications. In other words, a buried cysteine residue is less likely to react with a Bq molecule in solution than an exposed one and the metalation caused the rest of the protein to fold even at low pH.

3.6. The Bq reaction profile of apo-α-rhMT when in solution with As-metalated MT species

The reaction profile for the reaction of Bq with all 11 free cysteines of the apo-α-MT is unlike that expected based on the low pH conditions. Based on our previous studies [11], it was expected that MT would not have a defined structure capable of interfering with the Bq cysteine modification reaction. At the low pH these spectra and titrations were carried out at 2.8, it was expected that the MT would exist in a denatured form, as a random, loosely defined structure, as depicted by the model in Fig. 3A. As such, all cysteine residues would be expected to exhibit a similar degree of steric hindrance towards the reactive Bq by the protein backbone and would be equally likely to react with the Bq molecule. This would result in a Normal distribution of the modifications with an increasing manifold maximum from apo- to the fully modified Bq_{11} species [11]. This was clearly not the case in the reaction profile of the α-MT species studied here. The presence of the As^{3+} changed the reaction mechanism for each species as seen from the modification distribution patterns in Fig. 2B, 2C and 2C.

While the reaction profiles for As_1-α-rhMT and As_2-α-rhMT are relatively straightforward to explain, the reaction profile of the apo-species in the presence of the As-bound protein is very much more difficult to interpret. At pH 2.8 it is unlikely that the apo-α-rhMT has much formal structure that should interfere or modify the accessibilities of the free cysteinyl thiols of the protein. In previous studies, fully metalated As-MT species have been shown to transfer As^{3+} to apo-species through protein–protein interactions. Many other studies have demonstrated MT donating metals such as Zn and Cu to other metalloenzymes through direct interaction with each other.

The pattern is not likely a result of Bq aggregation or some other property of the cysteine-Bq reaction because the pattern is not replicated in the absence of a bound metal. In solutions only containing apo-MT this phenomenon is not seen [11]. The presence of metal induced structure at pH 2.8 indicates that H-bonding may not be an important factor in determining As-MT structure. The pattern shown in Fig. 2D is very similar to the one in 2C. It is likely the interaction and transfer from the As_1 species to the apo-species is causing the altered reaction profile of Bq.

3.7. Models of apo-α-MT1a, As_1-α-MT1a and As_2–MT1a

The models were calculated using MM3/MD techniques at a nominal MD temperature of 500 K temperature to simulate a low pH environment with the H-bonds disrupted. The models suggest that apo is indeed the most open conformation of the protein and that when bound to arsenic, the protein adopts a somewhat globular structure. As described before, even though apo-MT may have an open, string-like structure at low pH, protein–protein interaction with partially metalated species may account for the Bq reaction profile resembling that of a structured protein. We suggest that the metalated species and apo-species interact with each other shielding the cysteine residues that are on the surface of both structures. The transfer of arsenic most likely occurs by a process of coordination of the As^{3+} by exposed cysteinyl thiols on the surface of an apo-protein [21]. This would explain the drastic change in reaction profile, since under metal-free conditions those most exposed residues would be the ones most likely to react with an incoming Bq molecule. The inter-protein exchange, therefore, maintains a pool of apo and minimally modified species by shielding the residues that under regular low pH conditions, would be the first to be modified. It should be noted that the most exposed residues at such a low pH would likely be closer to the end of the peptide and have less shielding from the backbone on one side when compared to the cysteine residues in the middle of the sequence. It is not known how great the difference would be between these two regions of the peptide at low pH.

Acknowledgments

We acknowledge financial support from the Natural Sciences and Engineering Research Council (DG and RTI grants), Academic Development Fund Grant at U.W.O. to M.J.S and OGSST (GWI). We thank Doug Hairsine for technical support with the mass spectrometer.

References

[1] D.H. Petering, J. Zhu, S. Krezoski, J. Meeusen, C. Kiekenbush, S. Krull, T. Specher, M. Dughish, Apo-metallothionein emerging as a major player in the cellular activities of metallothionein, Exp. Biol. Med. 231 (2006) 1528–1534.
[2] W. Braun, M. Vasak, A.H. Robbins, C.D. Stout, G. Wagner, J.H. Kagi, K. Wuthrich, Comparison of the NMR solution structure and the X-ray crystal structure of rat metallothionein-2, Proc. Natl. Acad. Sci. U.S.A. 89 (1992) 10124–10128.
[3] A.H. Robbins, D.E. McRee, M. Williamson, S.A. Collett, N.H. Xuong, W.F. Furey, B.C. Wang, C.D. Stout, Refined crystal structure of Cd, Zn metallothionein at 2.0 Å resolution, J. Mol. Biol. 221 (1991) 1269–1293.
[4] K.E. Rigby-Duncan, M.J. Stillman, Metal-dependent protein folding: metallation of metallothionein, J. Inorg. Biochem. 100 (2006) 2101–2107.
[5] M. Capdevila, R. Bofill, O. Palacios, S. Atrian, State-of-the-art of metallothioneins at the beginning of the 21st century, Coord. Chem. Rev. 256 (2012) 46–62.
[6] T. Fukada, S. Yamasaki, K. Nishida, M. Murakami, T. Hirano, Zinc homeostasis and signaling in health and diseases, J. Biol. Inorg. Chem. 16 (2011) 1123–1134.
[7] J. An, Y. Pan, Z. Yan, W. Li, J. Cui, Y. Jiao, L. Tian, R. Xing, Y. Lu, Mir-23a in amplified 19p13.13 loci targets metallothionein 2a and promotes growth in gastric cancer cells, J. Cell. Biochem. 114 (2013) 2160–2169.
[8] T. Otsuka, A. Hamada, K. Iguchi, S. Usui, K. Hirano, Suppression of metallothionein 3 gene expression by androgen in LNCaP prostate cancer cells, Biodmed. Rep. 1 (2013) 614–618.
[9] M. Vašák, Advances in metallothionein structure and functions, J. Trace Elements Med. Biol. 19 (2005) 13–17.
[10] K.E. Rigby, M.J. Stillman, Structural studies of metal-free metallothionein, Biochem. Biophys. Res. Commun. 325 (2004) 1271–1278.
[11] K.L. Summers, A.K. Mahrok, M.D.M. Dryden, M.J. Stillman, Structural properties of metal-free apometallothioneins, Biochem. Biophys. Res. Commun. 425 (2012) 485–492.
[12] D.H. Petering, J. Zhu, S.K. Krezoski, J. Meeusen, C. Kiekenbush, S. Krull, T. Specher, M. Dughish, Apo-metallothionein emerging as a major player in the cellular activities of metallothionein, Exp. Biol. Med. 231 (2006) 1528–1534.
[13] A. Arseniev, P. Schultze, E. Woergoetter, W. Braun, G. Wagner, M. Vasak, J.H.R. Kaegi, K. Wuthrich, Three-dimensional structure of rabbit liver [Cd7]metallothionein-2a in aqueous solution determined by nuclear magnetic resonance, J. Mol. Biol. 201 (1988) 637–657.
[14] D.A. Fowle, M.J. Stillman, Comparison of the structures of the metal-thiolate binding site in Zn(II)-, Cd(II)-, and Hg(II)-metallothioneins using molecular modeling techniques, J. Biomol. Struct. Dyn. 14 (1997) 393–406.
[15] G.W. Irvine, K.L. Summers, M.J. Stillman, Cysteine accessibility during As^{3+} metalation of the α- and β-domains of recombinant human MT1a, Biochem. Biophys. Res. Commun. 433 (2013) 477–483.
[16] D.E.K. Sutherland, M.J. Willans, M.J. Stillman, Supermetalation of the β domain of human metallothionein 1a, Biochemistry 49 (2010) 3593–3601.

[17] K.L. Bren, V.L. Pecoraro, H.B. Gray, Metalloprotein folding, Inorg. Chem. 43 (2004) 7894–7896.
[18] K.E.R. Duncan, M.J. Stillman, Evidence for noncooperative metal binding to the a domain of human metallothionein, FEBS J. 274 (2007) 2253–2261.
[19] M.E. Merrifield, J. Chaseley, P. Kille, M.J. Stillman, Determination of the Cd/S Cluster Stoichiometry in Fucus vesiculosus Metallothionein, Chem. Res. Toxicol. 19 (2006) 365–375.
[20] K.E.R. Duncan, M.J. Stillman, Kinetic and molecular dynamics studies on the metal-dependent folding of metallothionein (MT), FASEB J. 20 (2006) A501.
[21] T.T. Ngu, M.D. Dryden, M.J. Stillman, Arsenic transfer between metallothionein proteins at physiological pH, Biochem. Biophys. Res. Commun. 401 (2010) 69–74.